THE ASTROPHYSICAL JOURNAL, 303:280–291, 1986 April 1

PROBING THE MAGNETIC FIELD OF RADIO PULSARS: A REEXAMINATION OF POLARIZATION POSITION ANGLE SWINGS

JOHN J. BARNARD[1]
Laboratory for High Energy Astrophysics, NASA Goddard Space Flight Center
Received 1985 July 15; accepted 1985 September 30

ABSTRACT

We calculate the polarization position angle as a function of pulse longitude and polarization limiting radius in radio pulsars assuming a vacuum magnetic field. We also estimate the polarization radius, r_{pl}, based on the calculations of Cheng and Ruderman and Stinebring. We find that for rotation periods $P < 0.06$ s $r_{pl} \approx 2 \times 10^5 (P/1\ \mathrm{s})^{-2}$ cm and for $P > 0.06$ s $r_{pl} \approx 9 \times 10^8 (P/1\ \mathrm{s})^{0.4}$ cm for a surface magnetic field strength of 10^{12} G and radio frequency of 10^9 Hz. For short rotation periods, r_{pl} approaches the light cylinder radius, r_{lc}. Here the magnetic field becomes more azimuthal, and the excursion in position angle over a pulse is less, on average, than when $r_{pl} \ll r_{lc}$. We calculate the average change in position angle and find consistency with the observations, as summarized by Narayan and Vivekanand. This work provides an alternative to their "elliptical beam" hypothesis. Our interpretation is further supported by the frequency dependence of polarization angle swing in the Crab pulsar, and the frequency of single, double, and multiple pulse components, and is consistent with the number of observed pulsars in plerions.

Subject headings: polarization — pulsars — stars: magnetic

I. INTRODUCTION

Current models of radio pulsars (e.g., Ruderman and Sutherland 1975; Arons and Scharlemann 1979; Arons 1983) predict an outflowing electron-positron plasma through which radio waves propagate. Propagation through this plasma should have several observational consequences (see, e.g., Melrose and Stoneham 1977; Melrose 1979; Cheng and Ruderman 1979, hereafter CR; Blandford and Scharlemann 1976; Stinebring 1982; Barnard and Arons 1986, hereafter BA). In particular, it has been found that the polarization state of the radio emission will be fixed at a polarization limiting radius r_{pl} (Melrose and Stoneham 1977; CR; Stinebring 1982) where the two wave modes subsequently maintain a nearly fixed phase relationship and thus maintain a nearly constant polarization state. In this paper we examine the magnitude of r_{pl} and find that at some radio frequencies, pulsar rotation periods P, and surface magnetic field strengths B_s, this may occur at distances comparable to the light cylinder radius, r_{lc}. As this radius is approached the field lines become quite swept back, exhibiting an increasingly azimuthal nature. When $r_{pl} \approx r_{lc}$, the familiar S-shaped swing in polarization angle (see Radhakrishnan and Cooke 1969; Manchester and Taylor 1977) will be modified. Since $r_{pl} \approx r_{lc}$ implies that the field will become more uniform where the polarization is fixed, the polarization angle will typically undergo a smaller swing. Recently, Narayan and Vivekanand (1983, hereafter NV; see also Jones 1980) have found that in fact the average swing in polarization position angles is less than expected from a rotating magnetic dipole with a circular emission cone at short rotation periods. They concluded that the cones are highly elliptical with small axis perpendicular to the rotation axis. Electrodynamic models suggest that the beams should be roughly circular (see, e.g., Ruderman and Sutherland 1975 or Barnard and Arons 1982), or kidney shaped with widest dimension oppositely oriented to that of NV (as in Arons and Scharlemann 1979). In this paper we examine the consequences of azimuthal fields for pulsar polarization swings quantitatively, and suggest that Narayan and Vivekanands's observation is a result of the effects of the rotationally induced azimuthal fields. In § II we calculate the position angle as a function of pulse longitude for several values of the polarization limiting radius r_{pl} assuming that the magnetic field is that due to the vacuum rotator (as in Deutsch 1955) and indicate the modifications to the calculation when a more realistic wind model is used. In § III, we estimate r_{pl} as a function of P, B_s, radio frequency ν, and plasma parameters, using the results of Melrose (1979), Stinebring (1982), and CR.

In § IV we calculate average polarization swings and compare with those found by NV. In § V we discuss the frequency dependence of position angle swing and compare with the Crab pulsar—the pulsar with observations of position angle covering many decades in frequency.

II. POLARIZATION POSITION ANGLE

a) *Geometry of Position Angle Swing*

Current work on pulsar emission and transfer mechanisms (e.g., Melrose 1979; CR; Stinebring 1982; Arons and Barnard 1986; BA) all have in common the fact that the polarization state of the radio (or higher frequency emission) will be such as to be either parallel or perpendicular to the projection of the local magnetic field onto the plane perpendicular to the line of sight to the pulsar when $r < r_{pl}$. In the following discussion, we will calculate the emission point as a function of pulse longitude by assuming that the dipolar magnetic field at emission point is parallel to the line of sight to the pulsar, which is conveniently done in the spherical coordinates aligned with the magnetic dipole. We then convert to Cartesian coordinates in the inertial frame and solve for the subsequent coordinates of the ray as a function of radius. Allowing for the finite travel time of the ray and the concurrent rotation of the pulsar, we may calculate the local magnetic field direction, at some given radius (i.e., at r_{pl}) and pulse longitude using a specified magnetic field. The projection of the field onto the plane perpen-

[1] National Research Council Resident Research Associate.

dicular to the line of sight then determines the polarization angle.

In order to calculate the position angle we choose a fiducial direction to be the projection of the rotation axis, $\mathbf{\Omega}$, onto the plane perpendicular to the direction of the line of sight, $\boldsymbol{n}$. We wish to calculate the angle ψ between this direction and the projected magnetic field. We construct a Cartesian coordinate system with z-axis along the rotation axis, and x-axis in the $(\boldsymbol{n}, \mathbf{\Omega})$ plane. Let α be the angle between $\boldsymbol{n}$ and $\mathbf{\Omega}$, and let $\boldsymbol{b}$ be the unit magnetic field vector. Then, as shown in BA:

$$\tan\psi = [1 - (\boldsymbol{b}\cdot\mathbf{\Omega})^2 - (\boldsymbol{n}\cdot\boldsymbol{b})^2 - (\boldsymbol{n}\cdot\mathbf{\Omega})^2 + 2(\boldsymbol{n}\cdot\boldsymbol{b})(\boldsymbol{n}\cdot\mathbf{\Omega})(\mathbf{\Omega}\cdot\boldsymbol{b})]^{1/2}/[\boldsymbol{b}\cdot\mathbf{\Omega} - (\boldsymbol{n}\cdot\boldsymbol{b})(\boldsymbol{n}\cdot\mathbf{\Omega})] \quad (1)$$

This can be considerably simplified to

$$\tan\psi = b_y(b_z\sin\alpha - b_x\cos\alpha)^{-1}\,, \quad (2)$$

If the emission occurs near enough to the star such that the magnetic field is to a good approximation that of a dipole, inclined by an angle i from the rotation axis, then the coordinates of the emission points of a ray that travels straight in the inertial frame are given by:

$$\tan\phi_d = (\sin\delta\sin\alpha)/(\cos i\ \sin\alpha\cos\delta - \sin i\cos\alpha),$$
$$\theta_d \approx \tfrac{2}{3}[(\alpha-1)^2 + \delta^2\sin^2\alpha]^{1/2}\,. \quad (3)$$

Here ϕ_d and θ_d are the azimuth and colatitude, respectively, of the emission point in spherical coordinates aligned with the (rotating) magnetic dipole, and δ is the azimuth of the dipole in the fixed laboratory frame. Note that for a given α, i, and δ, the emission radius r_e is arbitrary, whereas ϕ_d and θ_d are determined. Expressed in the fixed laboratory frame, the Cartesian coordinates (x_e, y_e, z_e) of the emission point are then

$$\begin{aligned} x_e &= (r_e\sin\theta_d\cos\phi_d\cos i + r_e\cos\theta_d\sin i)\cos\delta \\ &\quad - r_e\sin\theta_d\sin\phi_d\sin\delta\,, \\ y_e &= r_e\sin\theta_d\cos\delta \\ &\quad + (r_e\sin\theta_d\cos\phi_d\cos i + r_e\cos\theta_d\sin i)\sin\delta\,, \\ z_e &= r_e\cos\theta_d\cos i - r_e\sin\theta_d\cos\phi_d\sin i\,. \end{aligned} \quad (4)$$

If the rays travel straight paths in the inertial frame, the Cartesian coordinates (x, y, z) at radius r will be

$$\begin{aligned} x &= x_e + (z - z_e)\tan\alpha\,, \\ y &= y_e\,, \\ z &= \sin\alpha(z_e\sin\alpha - x_e\cos\alpha) \\ &\quad + \cos\alpha[r^2 - y_e^2 - (z_e\sin\alpha - x_e\cos\alpha)^2]^{1/2}\,. \end{aligned} \quad (5)$$

Equation (5) simply reflects the fact that all rays that reach the observer travel in planes parallel to the (x, z)-plane at an angle α from the z-axis.

The extremes in δ (δ_{max} and δ_{min}) for which the pulsar will be observed depend on i, α, and the half-angle of the cone of emission ξ_f:

$$\delta_{min} \approx \pm[\xi_f^2 - (\alpha - i)^2]^{1/2}/\sin\alpha\,. \quad (6)$$

b) *Specifying the Magnetic Field*

To calculate the excursion in ψ as δ varies between δ_{min} and δ_{max} for a given pulsar orientation (α and i) and emission cone half-angle ξ_f one needs to specify the radius r_{pl} at which the polarization is determined and the magnetic field orientation at that radius.

The self-consistent solution to the magnetic and electric field structure and the plasma distribution in that field has of yet not been obtained. An exact solution to the fields surrounding a rotating conducting sphere in vacuo was obtained by Deutsch (1955). Although this is probably a poor approximation to the electric fields near a pulsar (since the plasma can easily short out much of the parallel electric field), the magnetic field should be well represented as long as the magnetic energy density exceeds the plasma energy density and the conduction currents are small.

The spherical components in Deutsch's solution can be written:

$$\begin{aligned} B_r &= B_0\left[\left(\frac{R}{r}\right)^3\cos i\cos\theta \right. \\ &\quad + \left(\frac{R}{r}\right)^2\left(\frac{R\Omega}{c}\right)\sin i\sin\theta\sin(\zeta+\lambda) \\ &\quad \left. + \left(\frac{R}{r}\right)^3\sin i\sin\theta\cos(\zeta+\lambda)\right], \\ B_\theta &= \frac{1}{2}B_0\left\{\left(\frac{R}{r}\right)^3\cos i\sin\theta + \left[\left(\frac{R\Omega}{c}\right)^2\left(\frac{R}{r}\right) - \left(\frac{R}{r}\right)^3\right]\right. \\ &\quad \times\sin i\cos\theta\cos(\zeta+\lambda) - \left(\frac{R\Omega}{c}\right)\left(\frac{R}{r}\right)^2 \\ &\quad \left.\times\sin i\cos\theta\sin(\zeta+\lambda)\right\}, \\ B_\phi &= -\frac{1}{2}B_0\sin i\left\{\left(\frac{R\Omega}{c}\right)\left(\frac{R}{r}\right)^2\cos(\zeta+\lambda)\right. \\ &\quad \left. + \left[\left(\frac{R\Omega}{c}\right)^2\left(\frac{R}{r}\right) - \left(\frac{R}{r}\right)^3\right]\sin(\zeta+\lambda)\right\}. \end{aligned} \quad (7)$$

Here B_0 is an arbitrary normalization, $\zeta \equiv r\Omega/c$, $\lambda \equiv \phi - \Omega t$, $\Omega \equiv |\mathbf{\Omega}|$, and t is the time such that the dipole is in the $(\boldsymbol{n}, \mathbf{\Omega})$-plane when $t = 0$. For a ray emitted in the direction of the observer $t \approx \delta/\Omega + (R - r_e)/c$. Equation (7) is approximate in that it assumes $(R\Omega/c) \ll 1$, which is a good approximation even for millisecond pulsars. Here R is the radius of the star taken throughout this paper to 10^6 cm.

Equation (7) should be valid (if conduction currents are small) if $r < r_a$, where r_a is the Alfvén radius, i.e., the radius at which the particle kinetic energy density is equal to the magnetic field energy density.

An estimate of r_a can be obtained from polar cap-pair creation models as in Ruderman and Sutherland (1975), Arons and Scharlemann (1979), or Arons (1983). As discussed in, for example, Arons and Barnard (1986) the kinetic energy density T can be estimated as

$$T = \epsilon n_0\, e\Delta\phi(n/n_0)\,. \quad (8)$$

Here $e\Delta\phi \approx e(R\Omega/c)^2 B_s R$ is the total polar cap potential available for particle acceleration, ϵ is the fraction of $e\Delta\phi$ actually obtained (which is less than unity due to pair formulation), n_0 is the particle density at the surface and is approximately equal to the corotation density, and B_s is the surface magnetic field at the pole. The quantity n/n_0 is proportional to the magnetic

field strength interior to the light cylinder radius (and so $\sim r^{-3}$), but exterior to r_{lc} the nearly radial trajectories of the particles leads to a r^{-2} dependence.

Equating T to the magnetic energy density $U = B^2/8\pi$ yields

$$r_a = \begin{cases} (1/4\epsilon)^{1/3} r_{lc} & \text{for } \frac{1}{4} < \epsilon < 1 \\ (1/4\epsilon) r_{lc} & \text{for } \epsilon < \frac{1}{4} \end{cases} . \quad (9)$$

Factors of order unity have been dropped in evaluating (8), and so the condition that $\epsilon = \frac{1}{4}$ for r_a to equal r_{lc} is somewhat oversimplified. We note that $r_a \approx r_{lc}$ unless $\epsilon \ll 1$.

For $r > r_a$, the plasma flows in a nearly radial direction, and the magnetic field will be that of a "wind" rather than of a vacuum "wave" as indicated in equation (7). As in the case of the solar wind, the condition of flux freezing leads to a primarily azimuthal field. The field line equation is

$$\frac{dr}{B_r} = \frac{r d\theta}{B_\theta} = \frac{r \sin\theta d\phi}{B_\phi} . \quad (10)$$

A frozen-in field implies that a field line that is anchored at a particular point on a surface that is corotating with the neutron star at $r = r_{lc}$ will pass through the locus of all points at which there is plasma which has passed through that particular point. Geometrical considerations show that a field line so constructed satisfies $d\theta/dr = \chi(\theta_{lc}, \phi_{lc})(r_{lc}/r)^2$ (assuming slight nonradial flow at $r = r_{lc}$). Also it can be shown that $d\phi/dr \approx -\Omega/v$. Here θ and ϕ are the colatitude and azimuth at r of a field line originating at $\theta = \theta_{lc}$, $\phi = \phi_{lc}$, $r = r_{lc}$ at some specified time, χ is an arbitrary function, and v is the plasma velocity. Conservation of radial magnetic flux requires that

$$B_r \approx B_r(\theta_{lc}, \phi_{lc}, r_{lc})(r_{lc}/r)^2 . \quad (11)$$

Thus using equations (10) and (11), the other two components may be written (in the limit $r \gg r_{lc}$):

$$B_\theta = B_r(r_{lc}, \theta_{lc}, \phi_{lc})\chi(\theta_{lc}, \phi_{lc})(r_{lc}/r)^3 , \quad (12)$$

$$B_\phi = -B_r(r_{lc}, \theta_{lc}, \phi_{lc})(r\Omega/v)(r_{lc}/r)^2 \sin\theta$$

$$\approx -B_r(r_{lc}, \theta_{lc}, \phi_{lc}) \sin\theta (r_{lc}/r) . \quad (13)$$

Comparison of equations (11)–(13) with equation (7) shows that for $r > r_{lc}$, $B_\phi \approx B_s(R\Omega/c)^2(R/r)$ and $B_r \approx B_s(R\Omega/c)(R/r)^2$ for both wind and wave magnetic fields. It is only B_θ which differs substantially in the two solutions: in the wave $B_\theta = B_s(R\Omega/c)^2(R/r)$, and in the wind $B_\theta \approx B_s(R/r)^3$.

c) *Evaluation of* $\Delta\psi$

We have evaluated ψ as a function of pulse longitude, assuming that the polarization is fixed at r_{pl}, for a number of values of r_{pl}, using the magnetic field of a vacuum wave (eq. [7]). This has been done numerically using equations (2)–(7) and the appropriate coordinate transformations between spherical and Cartesian coordinates. A typical example of the polarization position angle swing is displayed in Figure 1. As can be seen for $r \ll r_{lc}$, the swing reproduces, as expected, the standard S-shaped swing. However, for $r \approx r_{lc}$ the polarization angle is nearly constant across the pulse, while for $r \gg r_{lc}$ the change in position angle increases somewhat.

We may estimate this swing in the regimes $r_{pl} \ll r_{lc}$ and $r_{pl} \gg r_{lc}$. For $r_{pl} \ll r_{lc}$, the position angle is roughly the same as the magnetic azimuth. Assuming that the angles δ, and $\alpha - i$ are much less than unity, equation (3) becomes

$$\tan\psi \approx \delta \sin\alpha/(\alpha - i) \quad (r_{pl} \ll r_{lc}) . \quad (14)$$

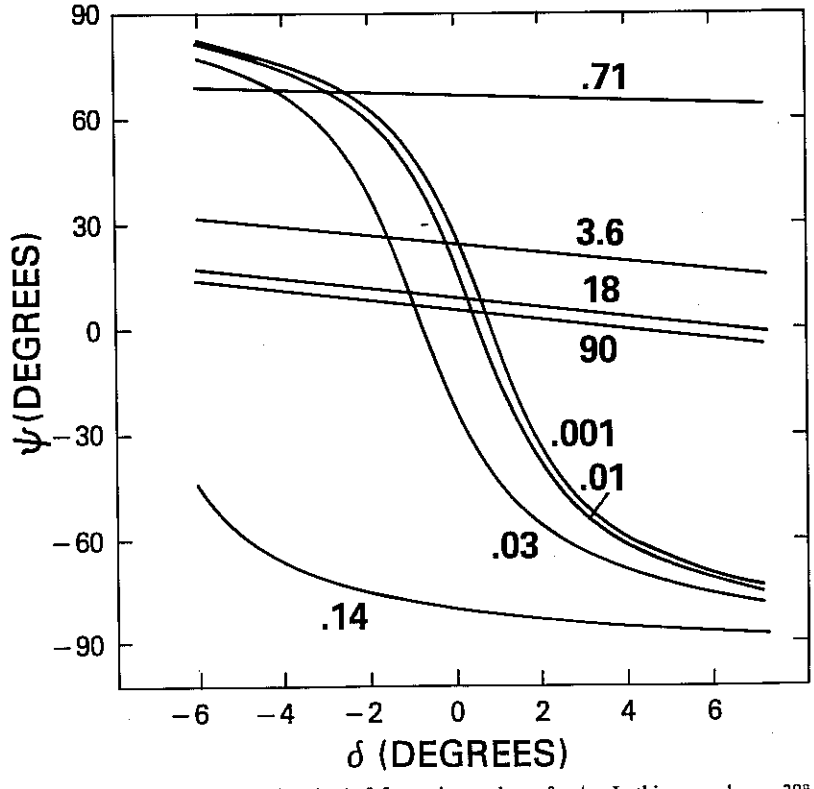

FIG. 1.—Polarization position angle ψ pulse longitude δ, for various values of r_{pl}/r_{lc}. In this example $\alpha = 39°$ and $i = 40°$.

For $r_{pl} \gg r_{lc}$, equation (2) becomes approximately

$$\tan \psi \approx -B_\phi/B_\theta \quad (r_{pl} \gg r_{lc}) . \tag{15}$$

So that for the vacuum wave field

$$\tan \psi \approx -\delta/\cos \alpha \quad (r_{pl} \gg r_{lc}) . \tag{16}$$

Here we have approximated $\lambda + \zeta$ by $-\delta$ since $r_e \Omega/c \ll \delta_{max}$, and for $r_{pl} \gg r_{lc}$, $\phi \approx 0$ and $\cos \theta \approx \cos \alpha$.

Typically, then polarization swings in the wave field at large radii are reduced by those at small radii by a factor of $\sim(\alpha - i) \ll 1$.

In the wind field for $r_{pl} \gg r_{lc}$, equations (12), (13), and (15) yield

$$\tan \psi \approx \sin \alpha (r_{pl}/r_{lc})^2/\chi(\theta_{lc}, \phi_{lc}) . \tag{17}$$

Since the field lines are nearly azimuthal for $r_{pl} \gg r_{lc}$,

$$\left.\frac{\partial \chi}{\partial \delta}\right|_{r_{pl}} \ll \left.\frac{\partial \chi}{\partial \delta}\right|_{r_{lc}} .$$

χ thus changes very little over the pulse. Hence,

$$\Delta \tan \psi \to 0 \quad \text{as } r_{pl}/r_{lc} \to \infty \tag{18}$$

Here $\Delta \tan \psi$ is the net change in $\tan \psi$ over the pulse. The result in equation (18) depends on the fact that field lines from adjacent pulsar rotation angles have their origin at the same magnetic pole. However, for some radii an open field line from one pole at large radii becomes adjacent to the field line from the opposite pole, resulting in a 180° change in the magnetic field (since it is primarily azimuthal), over a small change in radius. However, the change in radius over which the polarization swings abruptly is small compared to the characteristic scale of plasma parameters ($\sim r_{pl}$). Thus, it is expected that equation (18) will be valid quite generally in the wind at large radius.

Comparison of equations (16) and (17) reveals that because of the much smaller θ-component of the magnetic field in the wind case polarization swings will be even smaller in the wind case than in the wave case.

III. ESTIMATE OF THE POLARIZATION LIMITING RADIUS, r_{pl}

a) *Basic Definition of* r_{pl}

An estimate of r_{pl} in radio pulsars has been made before by CR and Stinebring (1982), based on the analogous problem of determining the polarization-limiting altitude of waves in the Earth's ionosphere considered by Budden (1952) and others referenced therein. Our purpose here is to generalize their calculations somewhat in order to estimate the functional dependence of r_{pl} on P, B_s, and other parameters.

The basic criterion used to determine r_{pl} is

$$\Delta k(r_{pl}) s(r_{pl}) \approx 1 . \tag{19}$$

Here $\Delta k(r_{pl})$ is the magnitude of the difference between the X-mode and O-mode wave vectors at r_{pl} (see Arons and Barnard 1986 for a discussion of X- and O-mode dispersion properties), and $s(r_{pl})$ is defined as the scale length for change in polarization parameters at r_{pl}. A more precise definition by Budden (1952) defines s (in his paper the notation was ψ^{-1}) by

$$s = |i(1 - R_0^2)/(dR_0/dr)| , \tag{20}$$

where R_0 is the ratio of the $\boldsymbol{n} \times \boldsymbol{\Omega}$ to $(\boldsymbol{n} \times \boldsymbol{\Omega}) \times \boldsymbol{n}$ components (both complex) of the electric field of the ordinary mode. (Budden's criterion, analogous to eq. [19], for r_{pl} is to within a factor of order unity the same as eq. [19], provided that $\Delta k \gg r^{-1}$.)

CR and Stinebring 1982) differ somewhat in their evaluation of equation (20). There are two contributions to the rate of change of s: the change in direction of the magnetic field, and the change in the plasma parameters which determine R_0 in equation (20). If the modes are linearly polarized (as in the case of an electron-positron plasma in which the components have equal densities and Lorentz factors γ), then the change in polarization parameters is entirely due to rotation of the magnetic field. If ψ is the angle between the projection of the z-axis and the projection of the magnetic field onto the plane perpendicular to $\boldsymbol{n}$ then equation (20) can be shown to be

$$s = 1/|d\psi/dr| . \tag{21}$$

As found by CR, $|d\psi/dr|^{-1}$ is of order the radius of curvature, ρ, of the magnetic field lines (providing that the angle between the field line and $\boldsymbol{k}$ is greater than $1/\gamma$). Thus the CR criterion for r_{pl} is

$$\rho \Delta k \approx 1 . \tag{22}$$

Pulsar models predict, however, that the electron and positron densities are not exactly equal, and thus the polarization state will change just due to the changes in the strength of the magnetic field and changes in the density and velocity of the plasma. This provides another source for the change in R_0 in equation (20). Stinebring (1982) evaluated equation (20) due to these changes in plasma parameters and found

$$\begin{aligned} s &= (p^2 + g^2)/|pdg/dr - gdp/dr| , \\ g &= -\sum_\alpha \epsilon_\alpha \omega_{p\alpha}^2 (\cos \theta_b - \beta_\alpha) f_\alpha/\omega_{B\alpha}\omega , \\ p &= \sum_\alpha \omega_{p\alpha}^2 \sin^2 \theta_b f_\alpha/2\gamma_\alpha^3 \omega^2 (1 - \beta_\alpha \cos \theta_b^2) , \\ f_\alpha &= \omega_{B\alpha}^2/[\gamma_\alpha^2 \omega^2 (1 - \beta_\alpha \cos \theta_b)^2 - \omega_{B\alpha}^2] \\ &\equiv \omega_{B\alpha}^2/(\omega'^2 - \omega_{B\alpha}^2) , \\ \omega_{p\alpha}^2 &= 4\pi q_\alpha^2 n_\alpha/m_\alpha , \end{aligned} \tag{23}$$

Here $\omega_{B\alpha} = |q_\alpha| B/m_\alpha c$, $\epsilon_\alpha = q_\alpha/|q_\alpha|$, and $\gamma_\alpha = (1 - \beta_\alpha^2)^{-1/2}$ is the Lorentz factor, θ_b is the angle between $\boldsymbol{k}$ and $\boldsymbol{b}$, while q_α, m_α, and n_α are the charge, mass, and density, respectively, of particles of species α. Also as derived by Melrose (1979) or Stinebring (1982), $\Delta n \equiv (c/\omega)\Delta k$ is given by

$$\Delta n = (p^2 + g^2)^{1/2} . \tag{24}$$

For simplicity we choose to calculate the contribution to p and g only from the electron-positron plasma. (See Stinebring 1982 for discussion of the effects of an energetic ion and positron beam). The quantity g can be rewritten

$$g = \frac{4\pi c}{\omega B} \sum_\alpha \eta_\alpha f_\alpha (\cos \theta_b - \beta_\alpha) . \tag{25}$$

Here η_α is the charge density of species α. If the positron and electron component each are characterized by the same γ, then g is further simplified to

$$g = 4\pi c (\cos \theta_b - \beta) f\eta/\omega B . \tag{26}$$

Here f is f_α evaluated for α either an electron or positron component of the plasma, and η the net charge density is obtained by assuming force free conditions are maintained (see Cheng

and Ruderman 1977). Note that $\eta = g = 0$ for equal number densities of electrons and positrons.

Similarly p can be estimated for an electron-positron plasma:

$$p = \frac{\omega_p^2 \sin^2 \theta_b f}{2\gamma^3 \omega^2 (1 - \beta \cos \theta_b)^2} . \quad (27)$$

In equations (22), or equations (23)–(27), evaluation of the quantities requires specifying the radial dependence of B, ω_p^2, γ, and $\theta_b \approx n_\perp$. Here $n_\perp$ is the component of $\boldsymbol{n}$ perpendicular to $\boldsymbol{B}$, where $\boldsymbol{n} = c\boldsymbol{k}/\omega$.

b) *Evaluation of* $r_{\rm pl}$

Our objective is to obtain the rough period and magnetic field dependence of $r_{\rm pl}$. We thus choose to evaluate quantities approximately in regimes where they are proportional to a power in the radius and identify the boundaries of these regimes. There are three characteristic radii which are of note. We define $r_{\omega B}$ as the cyclotron resonance radius such that $\omega' = \omega_B$, where ω' is the wave frequency in the frame comoving with the plasma of Lorentz factor γ. The light cylinder radius $r_{\rm lc}$ divides the dipolar magnetic field from the pulsar wave (or wind) field and the density profile from an r^{-3} to an r^{-2} dependence. And, for radii greater than approximately $(\xi_f/2)r_{\rm lc}$, $n_\perp$ and the radius of curvature of the magnetic field lines ρ are dominated by light cylinder effects rather than by the dipole field.

We identify three possible cases:

Case I:

$$r_{\omega B} < (\xi_f/2) r_{\rm lc} < r_{\rm lc} .$$

Case II:

$$(\xi_f/2) r_{\rm lc} < r_{\omega B} < r_{\rm lc} .$$

Case III:

$$(\xi_f/2) r_{\rm lc} < r_{\rm lc} < r_{\omega B} .$$

We find that except for very high wave frequencies and low magnetic field strengths cases II and III cover most parameters. We further breakdown cases II and III into subcases A, B, and C:

Case IIA:

$$(\xi_f/2) r_{\rm lc} < r_{\rm pl} < r_{\omega B} < r_{\rm lc} .$$

Case IIB:

$$(\xi_f/2) r_{\rm lc} < r_{\omega B} < r_{\rm pl} < r_{\rm lc} .$$

Case IIC:

$$(\xi_f/2) r_{\rm lc} < r_{\omega B} < r_{\rm lc} < r_{\rm pl} .$$

Case IIIA:

$$(\xi_f/2) r_{\rm lc} < r_{\rm pl} < r_{\rm lc} < r_{\omega B} .$$

Case IIIB:

$$(\xi_f/2) r_{\rm lc} < r_{\rm lc} < r_{\rm pl} < r_{\omega B} .$$

Case IIIC:

$$(\xi_f/2) r_{\rm lc} < r_{\rm lc} < r_{\omega B} < r_{\rm pl} .$$

In Tables 1, 2, and 3 we list the various quantities needed in order to evaluate equations (22) and (23). A few remarks are in order. The value of $n_\perp$ used in regions IIA, IIB, and IIIA reflects the increased azimuthal field from rotation. It is only for radii less than $(\xi_f/2)r_{\rm lc}$ that the value of $n_\perp$ will be determined by tracing rays through an essentially static magnetic dipole (as in BA). The charge density used in cases IIC, IIIB, and IIIC is calculated in the MHD approximation and using a radial flow velocity. That is,

$$\eta = \nabla \cdot \boldsymbol{E}/4\pi = \nabla \cdot (-\boldsymbol{v} \times \boldsymbol{B})/4\pi \approx \cot \theta (B_s/R)(R\Omega/c)^2 (R/r)^2 .$$

The other entries are typical of polar-cap, pair creation models of pulsars (e.g., Ruderman and Sutherland 1975; Arons and Scharlemann 1979). We take $\kappa \equiv 10^3 \kappa_3$; the number of pairs per primary particle and $\gamma (\equiv 10^2 \gamma_2)$ to be independent of P, an approximation to the weak period dependence found in pulsar models (see, e.g., Ruderman and Sutherland 1975; Arons and Scharlemann 1979; Daugherty and Harding 1982).

Using Tables 1, 2, and 3 we may solve for $r_{\omega B}$ and $r_{\rm pl}$. Solving $\omega' = \omega_B$ yields

$$\frac{r_{\omega B}}{R} = \begin{cases} 1050 B_{12}^{1/5} \nu_9^{-1/5} \gamma_2^{-1/5} P^{2/5} & \text{(case II)} \\ 1.25 B_{12} \gamma_2^{-1} \nu_9^{-1} P^{-2} & \text{(case III)} \end{cases} . \quad (28)$$

Here $B_{12} \equiv B_s/10^{12}$ G and $\nu_9 \equiv \nu/10^9$ Hz.

TABLE 1

EVALUATION OF QUANTITIES IN CASES II AND III

Quantity	$(\xi_f/2)r_{\rm lc} < r < r_{\rm lc}$	$r > r_{\rm lc}$
B	$B_s(R/r)^3 = 1.0 \times 10^{12} B_{12} (R/r)^3$ G	$B_s(R\Omega/c)^2(R/r) = 4.39 \times 10^4 B_{12} P^{-2}(R/r)$ G
γ	$100\gamma_2$	$100\gamma_2$
η	$\Omega B/2\pi c = 33.3 B_{12} P^{-1}(R/r)^3$ esu cm^{-3}	$(1/4\pi)(B_s/R)(R\Omega/c)^2(R/r)^2 \cot\theta =$ $3.48 \times 10^{-3} B_{12} P^{-2} \cot\theta (R/r)^2$ esu cm^{-3}
$\eta_\pm$	$\kappa\Omega B/2\pi ce = 6.9 \times 10^{13} \kappa_3 P^{-1} B_{12} (R/r)^3$ cm^{-3}	$(\kappa/2\pi e)(R\Omega/c)^2(B_s/R)(R/r)^2 =$ $1.45 \times 10^{10} P^{-2} \kappa_3 B_{12} (R/r)^2$ cm^{-3}
$(1 - \beta \cos\theta_b)$	$n_\perp^2/2 = (1/2)(R\Omega/c)^2(r/R)^2$ $= 2.2 \times 10^{-8} P^{-2}(r/R)^2$	1
$\cos\theta_b - \beta$	$-n_\perp^2/2 = -2.2 \times 10^{-8} P^{-2}(r/R)^2$	-1
$\sin\theta_b$	$n_\perp = (R\Omega/c)(r/R) = 2.9 \times 10^{-4} P^{-1}(r/R)$	1
ω	$2\pi\nu = 6.3 \times 10^9 \nu_9$ s^{-1}	$2\pi\nu = 6.3 \times 10^9 \nu_9$ s^{-1}
$\omega' = \gamma\omega(1 - \beta\cos\theta_b)$	$\gamma\omega n_\perp^2/2 = 1.38 \times 10^4 \gamma_2 \nu_9 P^{-2}(R/r)^2$ s^{-1}	$\gamma\omega = 6.3 \times 10^{11} \gamma_2 \nu_9$ s^{-1}
$\omega_p = (8\pi e^2 n_\pm/m)^{1/2}$	$6.63 \times 10^{11} \kappa_3^{1/2} P^{-1/2} B_{12}^{1/2} (R/r)^{3/2}$ s^{-1}	$6.5 \times 10^9 \kappa_3^{1/2} P^{-1} B_{12}^{1/2} (R/r)$ s^{-1}
$\omega_B = eB/mc$	$1.76 \times 10^{19} B_{12} (R/r)^3$ s^{-1}	$7.71 \times 10^{11} B_{12} P^{-2}(R/r)$ s^{-1}
ρ	$c/\Omega = 4.8 \times 10^9 P$ cm	$r = 10^6 (r/R)$ cm

TABLE 2

EVALUATION OF QUANTITIES IN CASE II

Quantity	A $(\xi_f/2)r_{lc} < r < r_{\omega B}$	B $r_{\omega B} < r < r_{lc}$	C $r_{lc} < r$
f	1	$\left(\frac{\omega_B}{\omega'}\right)^2 = 1.6 \times 10^{30} P^4 \gamma_2^{-2} \nu_9^{-2} \left(\frac{R}{r}\right)^2$	$\left(\frac{\omega_B}{\omega'}\right)^2 = 1.50 P^{-4} \gamma_2^{-2} \nu_9^{-2} B_{12}^2 \left(\frac{R}{r}\right)^2$
$p = \frac{\omega_p^2 \sin^2 \theta_b f}{2\gamma^3 \omega^2 (1 - \beta \cos^2 \theta)_b}$	$5.13 \times 10^5 \left(\frac{R}{r}\right)^5 P B_{12} \nu_9^{-2} \gamma_2^{-3} \kappa_3$	$8.44 \times 10^{35} \left(\frac{R}{r}\right)^5 P^5 B_{12}^3 \nu_9^{-4} \gamma_2^{-5} \kappa_3$	$1.76 \times 10^{-6} \left(\frac{R}{r}\right)^4 P^{-6} B_{12}^3 \nu_9^{-4} \gamma_2^{-5} \kappa_3$
$g = \frac{4\pi c n f (\cos \theta_b - \beta)}{B\omega}$	$4.35 \times 10^{-17} \left(\frac{R}{r}\right)^{-2} P^{-3} \nu_9^{-1}$	$7.19 \times 10^{13} \left(\frac{R}{r}\right)^8 P B_{12}^2 \nu_9^{-3} \gamma_2^{-2}$	$7.15 \times 10^{-6} \cot \theta \left(\frac{R}{r}\right)^3 P^{-4} B_{12}^2 \nu_9^{-3} \gamma_2^{-2}$

The division between cases II and III is thus:

$$\begin{aligned} P &> 0.06 B_{12}^{1/3} \nu_9^{-1/3} \gamma_2^{-1/3} \text{ s} \quad \text{(case II)} \\ P &< 0.06 B_{12}^{1/3} \nu_9^{-1/3} \gamma_2^{-1/3} \text{ s} \quad \text{(case III)} \end{aligned} . \tag{29}$$

The light cylinder radius is

$$\frac{r_{lc}}{R} = 4775 P . \tag{30}$$

The polarization limiting radius using the CR criterion becomes

$$\frac{r_{pl}}{R} = \begin{cases} 873 \kappa_3^{1/5} \gamma_2^{-3/5} \nu_9^{-1/5} B_{12}^{1/5} P^{2/5} \\ \qquad 2.4 > \kappa_3 \gamma_2^{-2} \quad \text{(case IIA)} \\ 991 \kappa_3^{1/15} \gamma_2^{-1/3} \nu_9^{-1/5} B_{12}^{1/5} P^{2/5} \\ \qquad 2.4 < \kappa_3 \gamma_2^{-2} \quad \text{(case IIB)} \\ 0.243 \kappa_3 \gamma_2^{-3} \nu_9^{-1} B_{12} P^{-2} \\ \qquad 5.1 > \gamma_2^{-2} \kappa_3 \quad \text{(case IIIA)} \\ 0.727 \kappa_3^{1/3} \gamma_2^{-5/3} \nu_9^{-1} B_{12} P^{-2} \\ \qquad 5.1 < \gamma_2^{-2} \kappa_3 \quad \text{(case IIIC)} \end{cases} \tag{31}$$

The solutions found for cases IIC and IIIA lie outside regions IIC and IIIA, respectively, for normal pulsar parameters.

To evaluate the Stinebring criterion for r_{pl} we let for each of cases IIA–IIIC

$$p \equiv p_0 (R/r)^{p_r} \prod_i \alpha_i^{p_\alpha} \quad g \equiv g_0 (R/r)^{g_r} \prod_i \alpha_i^{g_\alpha} ,$$

where each of the α_i are parameters such as B_{12}, ν_9, and so on, which are found in Tables 2 and 3, and where $\prod_i$ indicates the product of the various parameters.

Defining $Q \equiv (s\Delta k)^{-1}$, use of equation (23) implies

$$Q \equiv |(p_r - g_r)(c/R\omega)(R/r) pg| / (p^2 + g^2)^{3/2} ;$$

$$Q \approx \begin{cases} |p_r - g_r| (c/R\omega)(g_0/p_0^2)(R/r)^{1 + g_r - 2p_r} \prod_i \alpha_i^{g_\alpha - 2p_\alpha} \\ \qquad \text{if } p \gg g . \\ |p_r - g_r| (c/R\omega)(p_0/g_0^2)(R/r)^{1 + p_r - 2g_r} \prod_i \alpha_i^{p_\alpha - 2g_\alpha} \\ \qquad \text{if } g \gg p \end{cases} \tag{32}$$

Then r_{pl} is defined as the point where $Q = 1$. Solving for r_{pl}:

$$\frac{r_{pl}}{R} = \begin{cases} \left[\frac{1}{|p_r - g_r|} \left(\frac{R\omega}{c} \right) \frac{p_0^2}{g_0} \prod_i \alpha_i^{2p_\alpha - g_\alpha} \right]^{1/(2p_r - g_r - 1)} \\ \qquad \text{if } p \gg g \\ \left[\frac{1}{|p_r - g_r|} \left(\frac{R\omega}{c} \right) \frac{g_0^2}{p_0} \prod_i \alpha_i^{2g_\alpha - p_\alpha} \right]^{1/(2g_r - p_r - 1)} \\ \qquad \text{if } g \gg p \end{cases} \tag{33}$$

Thus we find the following solutions for $s\Delta k = 1$, using Stinebring's criterion and Tables 2 and 3:

$$\frac{r_{pl}}{R} = \begin{cases} 0.246 B_{12} \nu_9^{-1} \gamma_2^{-3} \kappa_3 P^{-2} \\ \qquad \text{(case IIIB and } p \gg g) \\ 856 B_{12}^{2/11} \kappa_3^{2/11} \gamma_2^{-6/11} \nu_9^{-2/11} P^{5/11} . \\ \qquad \text{(case IIA and } p \gg g) \\ 6.0 B_{12} \kappa_3^{-1} \gamma_2 \nu_9^{-1} P^{-2} \\ \qquad \text{(case IIIC and } p \ll g) \end{cases} \tag{34}$$

Again we have ignored those solutions which are inconsistent. The striking aspect of equations (31) and (34) is that both of

TABLE 3

EVALUATION OF QUANTITIES IN CASE III

Quantity	A $(\xi_f/2)r_{lc} < r < r_{lc}$	B $r_{lc} < r < r_{\omega B}$	C $r_{\omega B} < r$
f	1	1	$\left(\frac{\omega_B}{\omega'}\right)^2 = 1.50 P^{-4} \gamma_2^{-2} \nu_9^{-2} B_{12}^2 \left(\frac{R}{r}\right)^2$
$p = \frac{\omega_p^2 \sin^2 \theta_b f}{2\gamma^3 \omega^2 (1 - \beta \cos \theta_b)^2}$	$5.13 \times 10^5 \left(\frac{R}{r}\right)^5 P B_{12} \nu_9^{-2} \gamma_2^{-3} \kappa_3$	$1.17 \times 10^{-6} \left(\frac{R}{r}\right)^2 P^{-2} B_{12} \nu_9^{-2} \gamma_2^{-3} \kappa_3$	$1.76 \times 10^{-6} \left(\frac{R}{r}\right)^4 P^{-6} B_{12}^3 \nu_9^{-4} \gamma_2^{-5} \kappa_3$
$g = \frac{4\pi c n f (\cos \theta_b - \beta)}{B\omega}$	$4.35 \times 10^{-17} \left(\frac{R}{r}\right)^{-2} P^{-3} \nu_9^{-1}$	$4.77 \times 10^{-6} \cot \theta \left(\frac{R}{r}\right) \nu_9^{-1}$	$7.15 \times 10^{-6} \left(\frac{R}{r}\right)^3 P^{-4} B_{12}^2 \nu_9^{-3} \gamma_2^{-2} \cot \theta$

them display nearly the same period dependence and are close in magnitude to the cyclotron resonance radius equation (28). Physically this is partly a result of the rapid decline in the difference in indices of refraction on passing cyclotron resonance. For $r < r_{\omega B}$ (and $r < r_{lc}$), $\Delta n \propto \omega_p^2 \propto r^{-3}$, while for $r > r_{\omega B}$, $\Delta n \propto \omega_p^2 B^2 \propto r^{-9}$. This very sharp radial dependence leads to a polarization limiting radius which is a fraction of $r_{\omega B}$. We have plotted r_{pl} as a function of period in Figure 2, indicating the results of both the Stinebring and CR criteria. We note that for $P \sim 0.06$ s, $r_{pl} \approx r_{lc}$ for $B_s = 10^{12}$ G and $\nu = 10^9$ Hz. It is apparent, then, that for short rotation periods the azimuthal components of the magnetic field will be reflected in the polarization data.

IV. CHANGE IN POSITION ANGLE AVERAGED OVER ORIENTATION ANGLES

a) $\langle \Delta\psi \rangle$ as a function of r_{pl}

The results of § II allow us to calculate the change in position angle, $\Delta\psi$, which should occur during one pulse, given some r_{pl}. However, for any given pulsar it is difficult to distinguish between a polarization swing in which $r_{pl} \approx r_{lc}$ and one in which $|\alpha - i| \approx \xi_f$, since both will result in small excursions in position angle. We wish therefore to calculate the average $\Delta\psi$ expected from a large number of pulsars viewed from random angles.

The average change in polarization angle $\langle \Delta\psi \rangle$ for a group of potentially observable pulsars with the same r_{pl} can be written

$$\langle \Delta\psi(r_{pl}) \rangle = \int_0^\pi di f_i(i) \int_0^\pi d\alpha f_\alpha(\alpha) \Delta\psi(\alpha, i, r_{pl}) P(i, \alpha, r_{pl})/N \, . \tag{35}$$

Here $f_i\, di$ is the fraction of potentially observable pulsars (with polarization limiting radius r_{pl}), with i between i and $i + di$, while $f_\alpha\, d\alpha$ is the fraction of pulsars, with α between α and $\alpha + d\alpha$, and $P(i, \alpha, r_{pl})$ is the probability of observing a pulsar with a given i and α. Here N is the normalization integral

$$N = \int_0^\pi di f_i(i) \int_0^\pi d\alpha f_\alpha(\alpha) P(i, \alpha, r_{pl}) \, . \tag{36}$$

For a randomly distributed line of sight,

$$f_\alpha(\alpha) = \tfrac{1}{2} \sin \alpha \, . \tag{37}$$

The distribution of the angle between the rotation and magnetic axes is unknown. There is neither a theoretical nor observational consensus on whether i increases or decreases with time (see Ghosh 1984, and references therein). As a first guess we assume that i is also randomly distributed:

$$f_i(i) = \tfrac{1}{2} \sin i \tag{38}$$

Since $\Delta\psi$ is rather insensitive to i we expect the average $\Delta\psi$ to reflect this insensitivity, barring some malevolent distribution in i.

We assume pulsars all emit in a well-defined cone of half-angle ξ_f. That is, we assume a constant intensity for polar

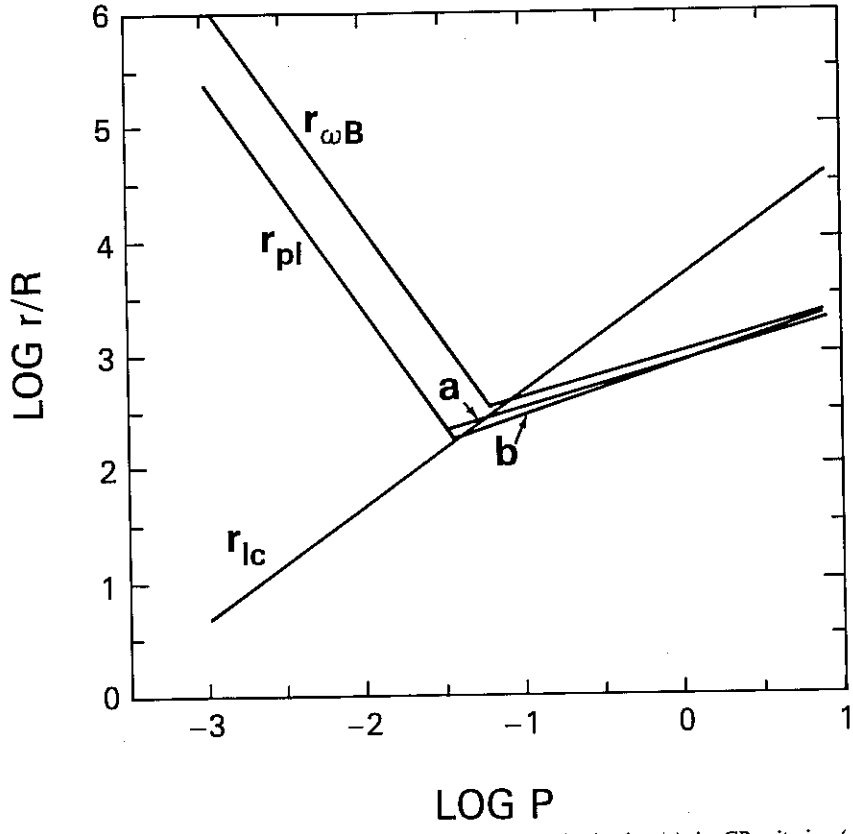

FIG. 2.—Polarization limiting radius r_{pl} vs. pulsar rotation period P. Solutions for r_{pl} obtained using (*a*) the CR criterion ($\rho\Delta k = 1$) and (*b*) the S criterion ($s\Delta k = 1$; see eq. [23]). Also shown are the cyclotron resonance radius $r_{\omega B}$ and light cylinder radius r_{lc}. Here $B_{12} = \gamma_2 = \nu_9 = \kappa_3 = 1$.

beaming angles less than ξ_f. The results will also be valid for a hollow cone of emission with outer angular radius ξ_f and should be approximately valid for any axisymmetric distribution with characteristic emission angle ξ_f.

For a potentially observable pulsar to be observed, $\xi_f > |\alpha - i|$. Hence

$$P(i, \alpha, r_{pl}) = \begin{cases} 1 & \text{if } \xi_f > |\alpha - i| \\ 0 & \text{if } \xi_f < |\alpha - i| \end{cases} . \quad (39)$$

Using equations (36)–(39) yields

$$N = (\tfrac{1}{4})\pi\xi_f + O(\xi_f^3) . \quad (40)$$

We have calculated numerically $\langle \Delta\psi \rangle$ as a function of r_{pl}, using the results of § II and have plotted the results in Figure 3, for three different values of ξ_f. As can be seen for large values of r_{pl}, $\langle \Delta\psi \rangle$ is a sensitive function of ξ_f. We may independently estimate ξ_f by looking at average pulse widths ($=2\delta_{max}$). Analogous to equation (35), we have, using equation (6) and equations (35)–(39),

$$\begin{aligned} \langle 2\delta_{max} \rangle &= N^{-1} \int_0^\pi di f_i(i) \int_0^\pi d\alpha f_\alpha(\alpha) 2\delta_{max} P(i, \alpha, r_{pl}) \\ &\approx 2(\pi\xi_f)^{-1} \int_0^\pi di \sin i \int_{i-\xi_f}^{i+\xi_f} d\alpha [\xi_f^2 - (\alpha - i)^2]^{1/2} . \\ &\approx 2\xi_f + O(\xi_f^3) \end{aligned} \quad (41)$$

Thus, the simple result is that the average pulse width is equal to the angular diameter of the pulsar beam.

We may also estimate $\langle \Delta\psi \rangle$ in the two regimes of § IIc. For $r_{pl} \ll r_{lc}$, equation (14) and equations (35)–(40) yields

$$\begin{aligned} \langle \Delta\psi \rangle &= \frac{1}{4N} \int_0^\pi di \sin i \int_{i-\xi_f}^{i+\xi_f} d\alpha \sin \alpha \\ &\quad \times |2 \tan^{-1} \{[\xi_f^2 - (\alpha - i)^2]/(\alpha - i)\}| \\ &= 2 + O(\xi_f^2) \text{ rad} \approx 115^\circ \quad (r_{pl} \ll r_{lc}) . \end{aligned} \quad (42)$$

Here $\langle \Delta\psi \rangle$ is independent of ξ_f.

For the wave magnetic field, and $r_{pl} \gg r_{lc}$,

$$\begin{aligned} \langle \Delta\psi \rangle &= \int_0^\pi di \sin i \int_{i-\xi_f}^{i+\xi_f} d\alpha \sin \alpha \\ &\quad \times |2 \tan^{-1} \{[\xi_f^2 - (\alpha - i)^2]^{1/2}/\sin \alpha \cos \alpha]\}| . \end{aligned}$$

Extensive algebra leads to

$$\langle \Delta\psi \rangle \approx \xi_f[1 - \ln (4/\xi_f^2)] + \xi_f^3[\tfrac{7}{6} - \tfrac{5}{6} \ln (4/\xi_f^2)] + O(\xi_f^5) \quad (r_{pl} \gg r_{lc}; \text{ wave}) \quad (43)$$

And, in the case of the wind,

$$\langle \Delta\psi \rangle \to 0, \; r_{pl} \to \infty \quad (r_{pl} \gg r_{lc}; \text{ wind}) ;$$

b) $\langle \Delta\psi \rangle$ as a Function P

In § III we estimated r_{pl}, including its dependence on period. We may combine the results of §§ II*a* and III to produce a theoretical estimate of $\langle \Delta\psi \rangle$ as a function of rotation period. We have graphed $\langle \Delta\psi \rangle$ versus P for three different values of ξ_f using the CR criterion and setting the parameters B_{12}, γ_2, and

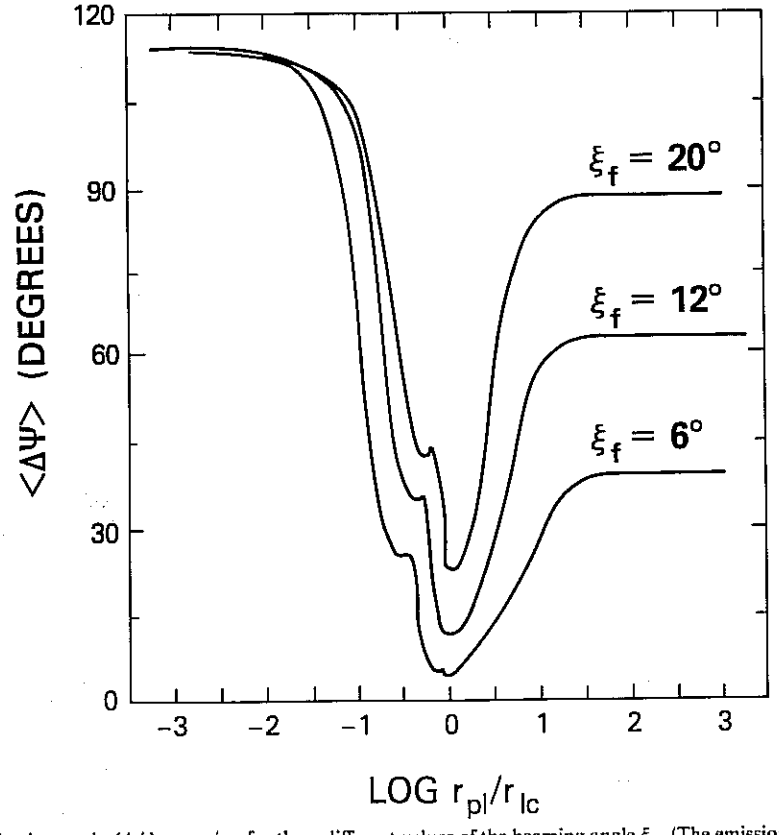

FIG. 3.—Average change in polarization angle $\langle \Delta\psi \rangle$ vs. r_{pl}/r_{lc}, for three different values of the beaming angle ξ_f. (The emission radius is assumed to be much less than r_{pl} or r_{lc}.)

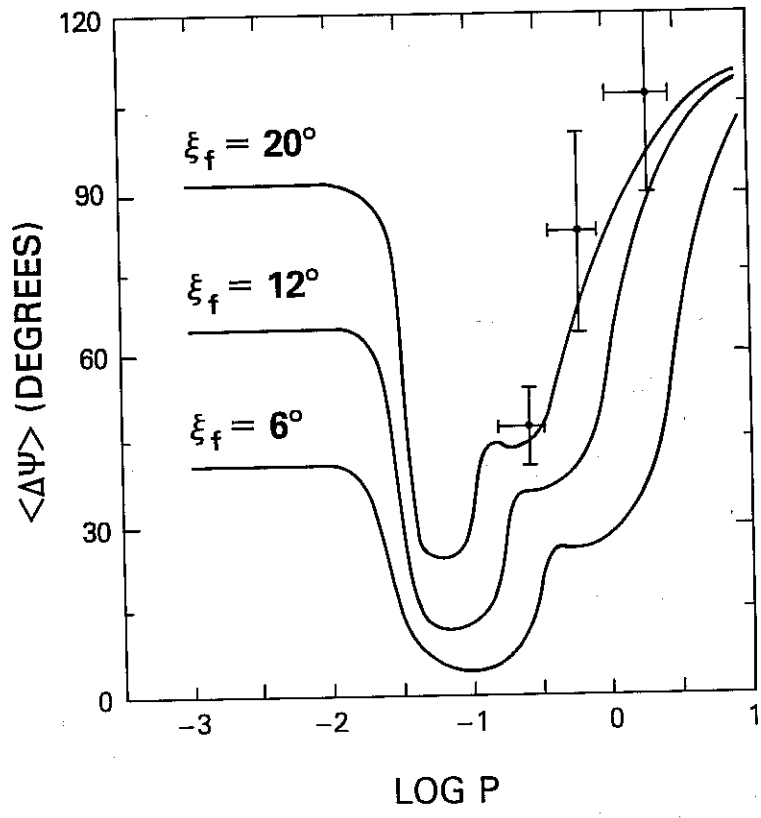

FIG. 4.—$\langle\Delta\psi\rangle$ vs. P, for three values of beaming angle, ξ_f. The quantity r_{pl} is estimated using the CR criterion, with $B_{12} = \gamma_2 = \kappa_3 = 1$, and $\nu_9 = 0.44$. Data points are from NV (see text).

κ_3 to 1, and ν_9 to 0.44 in Figure 4, and, with the same parameters except that $\gamma_2 = 3$, in Figure 5. We have also plotted the averages $\langle\Delta\psi\rangle$ using the data of NV. NV divided 30 pulsars with well-measured position angles into three groups of 10, according to rotation period. The averages and standard deviations for each group are

$$\langle P\rangle = 0.25 \pm 0.12 \text{ s}, \langle 2\delta_{max}\rangle = 21° \pm 12°, \quad \langle\Delta\psi\rangle = 46° \pm 28° .$$

$$\langle P\rangle = 0.59 \pm 0.24 \text{ s}, \langle 2\delta_{max}\rangle = 18° \pm 7°, \quad \langle\Delta\psi\rangle = 79° \pm 57° .$$

$$\langle P\rangle = 1.74 \pm 0.78 \text{ s}, \langle 2\delta_{max}\rangle = 10° \pm 9°, \quad \langle\Delta\psi\rangle = 105° \pm 50° .$$

The vertical error bars in Figures 4 and 5 reflect the standard deviation in $\langle\Delta\psi\rangle$ divided by 3.2, the square root of the number of points, while the horizontal error bars are the standard deviations in P giving an indication of bin size.

Since the average pulse widths together with equation (41) imply $\xi_f \approx 10°$, it is clear that Figure 5 (in which $\gamma_2 = 3$) represents a satisfactory fit to the data. In fact, if we define $\chi \equiv \kappa_3^{1/5}\gamma_2^{-3/5}B_{12}^{1/5}$, we find that $\chi \sim 0.5$ provides a good fit, indicating rough consistency of polar cap plasmas in a wave magnetic field with the observed polarization swings. Comparison of Figures 4 and 5 provides some indication of the sensitivity of $\langle\Delta\psi\rangle$ on the assumed value of the model parameters.

V. OBSERVING THE FREQUENCY DEPENDENCE OF $\Delta\psi$

For individual pulsars, this model predicts that the polarization swings should be weakly frequency dependent. However, as noted by Manchester (1971), a striking feature of radio pulsars is their frequency-independent polarization angles. Examination of equation (31) reveals why this is so. The majority of detailed polarization studies are at frequencies between 400 and 1600 MHz, a factor of 4 in frequency. Using the upper of equation (31), we see that this corresponds to only a 28% change in the polarization radius, which particularly for long-period pulsars, corresponds to an essentially undetectable change in polarization angle. Since the pulsars in NV cover two decades in period and because the period dependence is twice as sensitive as the frequency dependence, there is a 500% change in r_{pl} as P varies from 0.06 to 3 s, which makes the average position angle swing observably different over the range of observed periods.

There is one pulsar, however, the Crab pulsar, with polarization data separated by about six decades in frequency. The optical data (from Kristian *et al.* 1970) indicate a polarization swing of $\sim 180°$. Although the optical emission and radio emission are likely to have different emission mechanisms, the magnetic field should determine the position angle. The radio emission at 410 MHz (see Manchester 1971) changes position angle by 20°–30°, with uncertainties of that order. Equation (31) indicates that for the Crab pulsar $r_{pl} > r_{lc}$ for the radio regime but $r_{pl} \ll r_{lc}$ for the optical. The nearly coincident arrival times of the peak in the radio through γ-ray pulses argues for approximate spatial coincidence of the emission regions of various frequencies. The dramatically different change in position angle between optical and radio is consistent with the view presented here that r_{pl} is in two different magnetic field regimes.

Kristian *et al.* find that the approximate orientation angles for the Crab are $\alpha \approx 83°$ and $i \approx 90°$, consistent with observa-

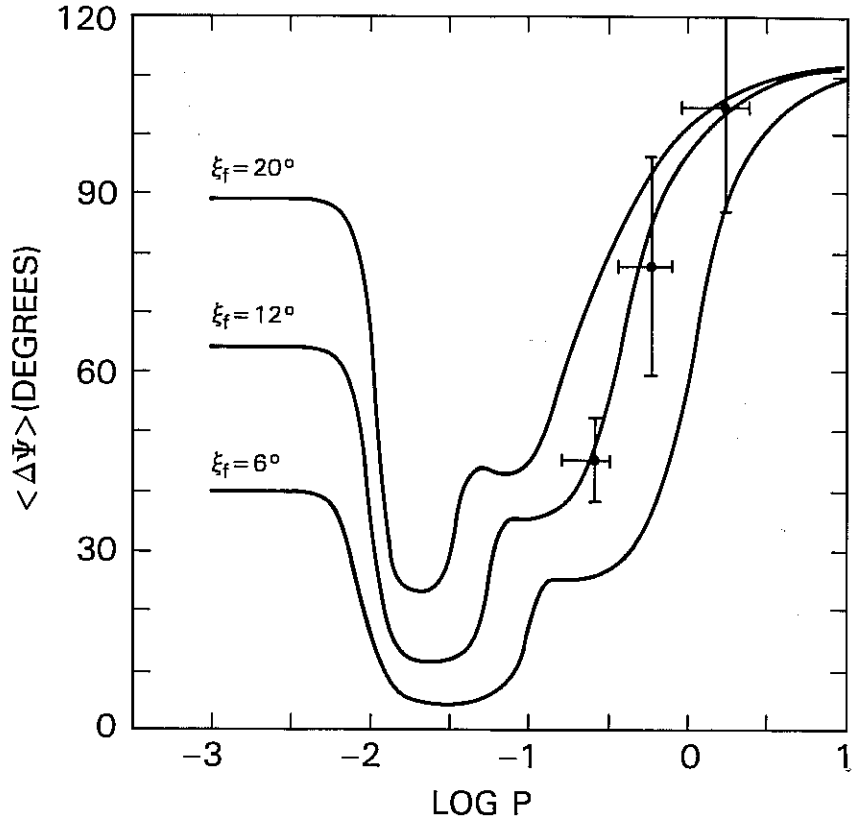

FIG. 5.—Same as Fig. 4, except that $\gamma_2 = 3$

tions of the interpulse, presumably originating from the opposite pole. It is interesting that for a vacuum wave for $i \approx \pi/2$, $\tan \psi \approx \delta/(\pi/2 - \alpha)$ for $r_{pl} \gg r_{lc}$, which is identical to the $r_{pl} \ll r_{lc}$ limit, indicating that a vacuum wave field will not fit the Crab field for $r_{pl} \gg r_{lc}$. This argues for being in the "wind" regime where $\tan \psi \to 0$ for $r_{pl} \gg r_{lc}$. However, absence of a more detailed magnetic field configuration prevents a detailed comparison of radio data with theory.

Other short-period pulsars may have $r_{pl} > r_{lc}$. For PSR 1937+21, $P = 1.6 \times 10^{-3}$ s and $B_{12} = 5 \times 10^{-4}$ (Backer, Kulkarni, and Taylor 1983). Equation (29) indicates that for this pulsar, below $\sim$26 GHz r_{pl} will be greater than r_{lc}. Stinebring (1983) and Stinebring and Cordes (1983) find that the polarization changes by $\sim$45° during each pulse component. This is a relatively small swing and is consistent with being in either the wind or dipolar zone. As indicated by equation (17), we expect $\Delta\psi$ to approach zero as ν_9 decreases, but as with the Crab the exact behavior requires a more detailed magnetic field model. The Vela pulsar ($P = 0.083$ s, $B_{12} \approx 3.3$) and PSR 1953+29 ($P = 6.1$, $B_{12} \approx 2.5 \times 10^{-3}$) both are predicted to have $r_{pl} \approx r_{lc}$. PSR 1953+29 is weakly polarized, and position angle data are not available (Stinebring *et al.* 1984). The Vela pulsar does show smaller $\Delta\psi$ as ν_9 decreases (Komesaroff, Morris, and Cooke 1970), but this has been shown to be a result of interstellar scattering (Komesaroff, Hamilton, and Ables 1972). After correcting for scattering they find no frequency dependence in position angle from 300–1400 MHz, to within the measurement errors. However, in all three of the above pulsars, high time resolution, pulse-by-pulse measurements are required to obtain accurate position angles and to remove the effects of "orthogonal modes" (see, e.g., Backer and Rankin 1980).

VI. DISCUSSION AND CONCLUSION

We estimated the polarization limiting radius (r_{pl}) using the results of Cheng and Ruderman 1980 (CR) and Stinebring 1982. We find that r_{pl} approaches r_{lc} if $P \sim 0.06$ s and $B_s \sim 10^{12}$ G. This manifests itself in the polarization data as a shallower swing in position angle. We have used the Deutsch (1954) magnetic field as a representation of the field interior to the light cylinder and estimate the effects of a wind exterior to the light cylinder. The observational data summarized by Narayan and Vivekanand (1983) are consistent with this work. However, their theoretical interpretation that pulsar beams are more elliptical at short periods is ad hoc, and it appears that these results can be explained more economically as a natural consequence of polar-cap, pair creation models, with approximately circular beams.

Roughly circular beams are also obtained by Backer (1976) who found, on the basis of the frequency of single- and double-pulse components, that the distribution of pulsar pulse components is consistent with having emission in circular hollow cones. Backer found that the ratio of pulsars with resolved double or complex pulses to those with simple or unresolved double pulses was about one to one. Binning the pulsars into the same period bins (with boundaries at 0.388 and 1.2 s), as was done for the polarization data, reveals that this ratio does not depend on period, within the statistical uncertainty. NV, however, find that the hollow portion of the cone of emission is roughly circular and does not depend on period. Their model

thus predicts a large ratio (>5:1) of simple to double or complex pulsars in the short-period bin. This is not supported in Backer's (1976) data.

Further, the apparent absence of pulsars in most plerions argues for a small beaming angle. The quantity N (cf. eq. [40]) is the fraction of 4π sr swept out by one pole of a pulsar averaged over α and i. If a pulsar has two emitting poles, then to order ξ_f^2 the fraction of pulsars which, on average, are beamed in our direction is given by $2N$. $\xi_f \approx 10°$ implies that $\sim 27\%$ of the sufficiently bright pulsar's may be seen, while NV would predict nearly 80% of the short-period pulsars would be observable given their ~ 5 to 1 ratio of major to minor axes. This assumes that the plerion-embedded pulsars are sufficiently bright to be detected. However, the very existence of plerions, i.e., supernova remnants with radio or X-ray emission distributed across the remnant, has been argued as evidence for young, luminous, pulsars (Weiler and Panagia 1978). Of the 13 known galactic plerions discussed by Seward (1982) (including W28, Kes 27, and W44), two are apparently accretion powered and are morphologically different than the other 11. Of the remaining 11, 10 are sufficiently nearby to contain observable pulsars. That is, if the Vela or Crab pulsar were placed in these remnants, they would have an observed flux above the sensitivity limits of the Jodrell Bank survey (see Davies, Lyne, and Seiradakis 1972) and second Molongolo survey (see Manchester *et al.* 1978). (3C 58, G74.9+1.2, and CTB 80 were not in the coverage of the latter survey, however.) Only three (30%) of the 10 contain observed pulsars (Crab, Vela, and MSH 14-52). Selection effects such as insensitivity to short-period pulsars, large-dispersion measures, and high background levels in the remnants have decreased the likelihood of observing pulsars in these remnants, however. Although the small fraction of plerionic pulsars is consistent with the small beaming angle hypothesis, the more sensitive surveys, such as described by Lyne (1984), are required to determine whether or not this small number is in fact due to selection effects.

NV argued that the preponderance of pulsars with interpulses to have short rotation periods is evidence for elongated beams at short periods. If pulsars have emission beamed from both magnetic poles, each with opening polar half-angle ξ_f (in the dipole-rotation axis plane), then the fraction of all pulsars N_i which are beamed in our direction and which have interpulses is given by

$$N_i = \int_{\pi/2-\xi_f}^{\pi/2} di \sin i \int_{\pi-i-\xi_f}^{\pi/2} d\alpha \sin \alpha \approx \xi_f^2/2 + O(\xi_f^4) . \quad (44)$$

Here we have assumed the same distributions in i and α as in equation (40) and have only included interpulses from opposite poles. Thus the fraction of observed pulsars with interpulses is $\sim N_i/(2N - N_i) \approx \xi_f/(\pi - \xi_f)$. If $\xi_f \approx 50°$ as suggested by NV for short-period pulsars, nearly 40% should have interpulses, while 5%–6% should for a 15°–20° beam diameter. Although NV found consistency with their beam model in their sample of 30 pulsars, when a larger sample is used the results are not as compelling. Of the 149 pulsars listed in Manchester and Taylor (1977), 35 have periods less than 0.38 s, 77 have periods between 0.388 and 1.2 s, and 37 have periods greater than 1.2 s. In the short-period group four are observed to have interpulses, while if $\xi_f = 10°$, 2 ± 1 are expected, and for $\xi_f = 50°$, 13 ± 4 would be expected. In the second group, only one is observed while 5 ± 2 are expected for $\xi_f = 10°$, and in the last group one is observed while 2 ± 1 should be present for the same ξ_f. Thus, there seems to be more of an underabundance of pulsars with interpulses at long period, than an overabundance of such pulsars at short period. This could be a consequence of pulsar alignment, rather than elongated beam size.

The assumed beam shape has consequences in determining the pulsar birth rate. Lyne, Manchester, and Taylor (1985) put the pulsar birth rate at one birth every 50 yr for a beaming angle of 15°, while a birth rate of one per 100 yr is implied if short-period pulsars have highly elongated beams. Both values are consistent with a supernova rate of about one per 30 yr (see Lyne, Manchester, and Taylor 1985, and references therein).

We have argued that further evidence for shallow polarization swings due to rotationally induced components to the magnetic field is found in the frequency dependence of the Crab polarization. The shallow polarization swing at radio frequencies contrasts to the nearly 180° swing at optical wavelengths. There is no obvious interpretation of these data in the elliptical beam model.

It has recently come to our attention that Shitov (1985) has also estimated rotational effects on pulsar polarization. Although using a different estimate of the rotationally induced magnetic field, he points out that the inflection point in the polarization curve (ψ vs. δ) will occur at values of δ which precede the center of symmetry of the pulse if the emission is at sufficiently high altitude. Our work shows that this effect also occurs if $r_{\rm pl}$ is sufficiently large (even though r_e may be small), as is verified in Figure 1. Shitov finds that a number of pulsars appear to demonstrate this effect and that it is most pronounced at short rotation periods.

Our results rely on a number of assumptions concerning the magnetic field and plasma parameters. In particular, we have ignored the effect of the polar current in changing the magnetic field direction of the polar field lines. At small $r_{\rm pl}$ this may have the effect of adding a small twist to the field lines, while for $r_{\rm pl} \rightarrow r_{\rm lc}$, the radio beam passes through field lines which contain a decreasing fraction of the current and so this effect may be minimal. We have also ignored plasma components other than the electron-positron component in determining $r_{\rm pl}$. Nevertheless, the calculations are consistent with the observations, and indicate that the magnetic field interior to $r_{\rm lc}$ may in a crude sense be approximated by the Deutsch model. Thus, we have shown that the polarization data can by these considerations be used as a probe of the magnetic field orientation in regimes quite removed from the radius where the radiation is emitted.

It is with pleasure that I thank A. K. Harding, J. Arons, D. Backer, D. Helfand, D. Stinebring, and the referee for useful suggestions and stimulating conversations. This work was supported by a National Research Council Resident Research Associateship at the Goddard Space Flight Center.

REFERENCES

Arons, J. 1983, *Ap. J.*, **266**, 215.
Arons, J., and Barnard, J. J. 1986, *Ap. J.*, **300**, in press.
Arons, J., and Scharlemann, E. T. 1979, *Ap. J.*, **231**, 854.
Backer, D. C. 1976, *Ap. J.*, **209**, 895.
Backer, D. C., Kulkarni, S. R., and Taylor, J. H. 1983, *Nature*, **301**, 314.
Backer, D. C., and Rankin, J. M. 1980, *Ap. J. Suppl.*, **42**, 143.
Barnard, J. J., and Arons, J. 1982, *Ap. J.*, **254**, 713.
———. 1986, *Ap. J.*, **301**, in press (BA).
Blandford, R. D., and Scharlemann, E. T. 1976, *M.N.R.A.S.*, **174**, 59.
Budden, K. G. 1952, *Proc. Roy. Soc. London, A*, **215**, 215.

Cheng, A. F., and Ruderman, 1977, *Ap. J.*, **212**, 800.
———. 1979, *Ap. J.*, **229**, 348 (CR).
Davies, J. G., Lyne, A. G., and Seiradakis, J. H. 1972, *Nature*, **240**, 229.
Daugherty, J. K., and Harding, A. K. 1982, *Ap. J.*, **252**, 337.
Deutsch, A. J. 1955, *Ann. d'Ap.*, **18**, 1.
Ghosh, P. 1984, *Astr. Ap.*, **5**, 307.
Jones, P. B. 1980, *Ap. J.*, **236**, 661.
Komesaroff, M. M., Hamilton, P. A., and Ables, J. G. 1972, *Australian J. Phys.*, **25**, 759.
Komesaroff, M. M., Morris, D., and Cooke, D. J. 1970, *Ap. Letters*, **5**, 37.
Kristian, J., Visvanathan, N., Westphal, J. A., and Snellen, G. H. 1970, *Ap. J.*, **162**, 415.
Lyne, A. G. 1984, in *NRAO Workshop 8, Birth and Evolution of Neutron Stars: Issues Raised by Millisecond Pulsars*, ed. S. P. Reynolds and D. R. Stinebring (Green Bank: NRAO), p. 223.
Lyne, A. G., Manchester, R. N., and Taylor, J. H. 1985, *M.N.R.A.S.*, **213**, 613.
Manchester, R. N. 1971, *Ap. J. Suppl.*, **23**, 283.
Manchester, R. N., Lyne, A. G., Taylor, J. H., Durdin, J. M., Large, M. I., and Little, A. G. 1978, *M.N.R.A.S.*, **185**, 409.
Manchester, R. N., and Taylor, J. H. 1977, *Pulsars* (San Francisco: Freeman).
Melrose, D. B., 1979, *Australian, J. Physics*, **32**, 61.
Melrose, D. B., and Stoneham, R. J. 1977, *Proc. Astr. Soc. Australia*, **3**, 120.
Narayan, R., and Vivekanand, M. 1983, *Astr. Ap.*, **122**, 45 (NV).
Radhakrishnan, V., and Cooke, D. J. 1969, *Ap. Letters*, **3**, 225.
Ruderman, M. A., and Sutherland, P. G. 1975, *Ap. J.*, **196**, 51.
Seward, F. D. 1982, in *IAU Symposium 101, Supernova Remnants and Their X-Ray Emission*, ed. J. Danziger and P. Gorenstein (Dordrecht: Reidel), p. 405.
Shitov, Y. P. 1985, *Astr. Zh.*, **62**, 54 (English trans., *Soviet Astr.*, **29**, 33 [1985]).
Stinebring, D. R. 1982, Ph.D. thesis, Cornell University.
———. 1983, *Nature*, **302**, 690.
Stinebring, D. R., Boriakoff, V., Cordes, J. M., Deich, W., and Wolszczan, A., 1984, in *NRAO Workshop 8, Birth and Evolution of Neutron Stars: Issues Raised by Millisecond Pulsars*, ed. S. P. Reynolds and D. R. Stinebring (Green Bank: NRAO), p. 32.
Stinebring, D. R., and Cordes, J. M. 1983, *Nature*, **306**, 349.
Weiler, K. W., and Panagia, N. 1978, *Astr. Ap.*, **70**, 419.

JOHN J. BARNARD: Code 665, Laboratory for High Energy Astrophysics, NASA Goddard Space Flight Center, Greenbelt, MD 20771